Eur. Phys. J. D **34**, 113–118 (2005)
DOI: 10.1140/epjd/e2005-00098-4

THE EUROPEAN PHYSICAL JOURNAL D

Tailoring the chemical reactivity and optical properties of clusters by size, structures and lasers

V. Bonačić-Koutecký[a], R. Mitrić, C. Bürgel, H. Noack, M. Hartmann, and J. Pittner[b]

Humboldt-Universität zu Berlin, Institut für Chemie, Brook-Taylor-Straße 2, 12489 Berlin, Germany

Received 6 September 2004

Abstract. We present results of theoretical investigations in three areas. I. Reactivity of anionic noble metal oxide clusters (Ag, Au) relevant for catalyst design: It will be shown that the cooperative effects are needed to activate clusters in order to invoke strongly size selective reactions with O_2 and CO. These results obtained with DFT method elucidated fully experimental findings. II. Stationary optical properties of silver clusters: ab initio results on absorption spectra of small silver clusters and on geometric relaxation of their excited states leading to the observed fluorescence are presented and compared with experimental data. III. Real-time investigation of ultrafast processes and their control by tailored laser fields: nonstoichiometric Na_nF_{n-1} clusters are suitable prototypes to study dynamics in excited electronic states. For this purpose we use our combination of the Wigner distribution method and MD "on the fly" allowing to treat all degrees of freedom. Analysis of simulated pump-probe signals will be shown for Na_2F for which experimental data are available. Pump-dump control of the photoisomerization in Na_3F_2 avoiding conical intersection will be presented using our new strategy for obtaining tailored laser fields based on the intermediate target in excited state which (if available) guarantees the controllability in the complex systems.

PACS. 31.15.Qg Molecular dynamics and other numerical methods – 31.15.Ar Ab initio calculations

1 Introduction

Nonscalable properties of atomic clusters in the size regime in which each atom counts [1–4] led to discoveries of many novel and unexpected phenomena with potential for applications in different technologies. These include: I. size selective reactivity of metal oxide clusters relevant for catalyst design; II. optical properties such as size and structure dependent absorption and fluorescence of metal clusters in context with optical data storage and III. analysis of ultrafast processes and their control by tailored laser fields driving reactions and photochemical processes towards the chosen product and suppressing other reaction pathways with possible applications in synthetic chemistry. In this contribution we present theoretical results for prototypes of the above mentioned research directions.

2 Results and discussion

2.1 Noble metal oxide clusters as model systems for heterogeneous catalysis

Although extensive information about catalytic activity of silver (e.g. oxidation reactions) is available the detailed reaction mechanism is unknown. Therefore the study of the interaction of silver particles with molecular oxygen aims to provide understanding of elementary catalytic reaction steps. Due to discovery of Haruta and coworkers [5] that nanosized gold particles can promote the oxidation of carbon monoxide, also oxidation of CO in the presence of gold has been a topic of increased interest [6,7]. In this context there are still numerous open questions regarding size and support effects, nature of the active site, mechanism for these reactions, influence of experimental conditions etc. One of the central issues which we will address here is whether the noble metal clusters are capable to break O_2 bond necessary for oxidation reactions or whether cooperative effects are needed to achieve this. We will show below that only in the latter case the reactions can occur.

In order to address this issue, we investigated (i) the multiple adsorption of molecular oxygen onto anionic silver clusters and (ii) the oxidation reaction of anionic gold

---

[a] e-mail: `vbk@chemie.hu-berlin.de`

[b] *Permanent address*: J. Heyrovský Institute of Physical Chemistry, Academy of Sciences of the Czech Republic, Dolejškova 3, 18223 Prague, Czech Republic.

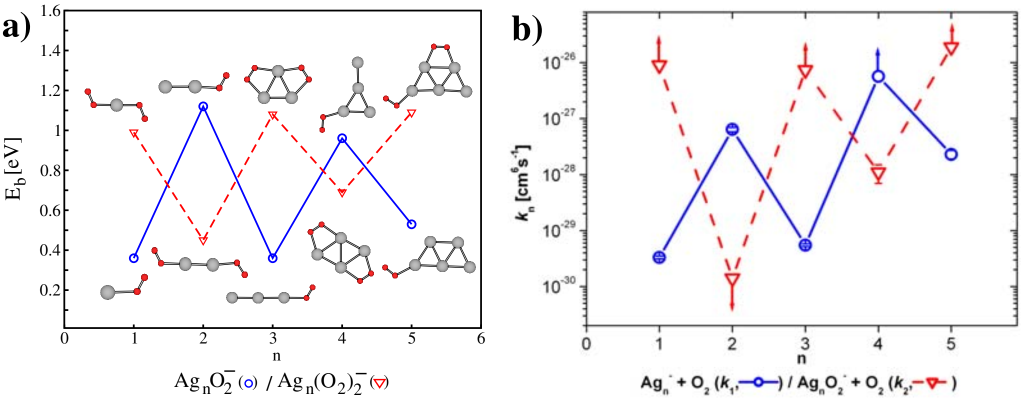

Fig. 1. (a) Theoretical binding energies E_b and lowest energy structures [20] and (b) experimental rate constants (T = 300 K) for adsorption of first (solid line) and second (dashed line) O_2 molecule onto Ag_{1-5}^-.

clusters with molecular oxygen and CO involving one and two CO molecules. The choice of the method for ground state properties is density functional method with appropriate functionals, e.g. B3LYP [8–10] and B3PW91 [8,11], allowing for calculation of reliable binding energies and energetics along the reaction pathways [12,13].

(i) Binding characteristics of molecular oxygen onto anionic silver clusters $Ag_n(O_2)_m^-$ (n = 1–5; m = 1, 2) [14] together with the most stable structures are shown in Figure 1a. The binding patterns exhibit a strong size dependent even-odd behaviour, which can be qualitatively explained in the framework of simple frontier orbital model. Anionic silver clusters with an even number of electrons (odd number of atoms), such as Ag^-, Ag_3^- and Ag_5^-, bind O_2 only weakly due to the closed shell structure in contrast to the open shell clusters, such as Ag_2^- and Ag_4^-. The binding of the first O_2 neutralizes anionic silver clusters and thus the inversion of the pattern occurs for the binding of the second O_2 molecule (Fig. 1a). This is due to the fact, that silver clusters have low VDEs and therefore one electron acceptor like O_2 can induce electron transfer from cluster to the π^* orbital of O_2 and activate the cluster leading to the strong cooperative binding with the second O_2. Therefore, in the case of Ag_3^- and Ag_5^- new oxide species with doubly bound superoxo-like O_2 subunits are stronger bound due to cooperative effects shown in Figure 1a and are activated for further oxidation reactions such as CO combustion.

These theoretical findings are in very good agreement with measured effective kinetic rate constants [14] shown in Figure 1b. A sequential adsorption mechanism is assumed with the effective rate constants k_1 for adsorption of first O_2 and k_2 for second O_2, which are largely determined by the binding energy E_b according to statistical rate theory. Notice that the rate constants differ in two orders of magnitude as a function of number of atoms confirming the pronounced effect of "each atom counts".

(ii) The role of molecular vs. dissociative chemisorption of oxygen onto gold cluster has been subject of many recent experimental and theoretical contributions [13,15–19], but the question remains, whether a gas-phase gold cluster can break the strong O=O bond of the O_2 molecule. The most stable structure of the prototype example $Au_2O_2^-$ binds oxygen in molecular superoxo-like form (r_{O-O} = 1.312 Å) (cf. Fig. 2). Along the pathway for the oxidation reaction, CO binds weakly to the gold atom with the O_2 group leading to the formation of complex III (cf. Fig. 2). This is followed by rearrangement with breaking of Au-O and formation of Au-C bond with low barrier leading to the intermediate complex IV with an OOCO group bound with the carbon atom to the Au_2 subunit. Starting from the intermediate complex IV two pathways are possible: (a) without cooperative effects (cf. dashed pathway in Fig. 2) and (b) with cooperative effects (solid pathway). In the absence of cooperative effects, the second CO molecule is not involved in the reaction mechanism representing experimental conditions in which only single CO molecule is involved. In order to emanate CO_2 under these conditions (cf. dashed pathway in Fig. 2), a barrier of about 0.649 eV (TS_4) has to be overcome, which is not feasible under thermal experimental conditions. However, the cooperative involvement of a second CO molecule opens new pathway (solid line in Fig. 2) with a lowered barrier. There, CO binds to gold and forms a O-C bond leading to formation of complex V

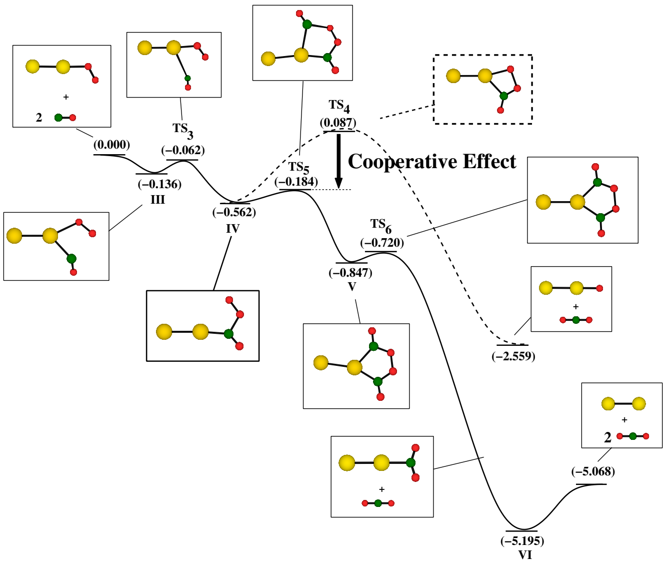

Fig. 2. Reaction profile for oxidation of CO by $Au_2O_2^-$ without (dashed pathway) and with cooperative effects (solid pathway).

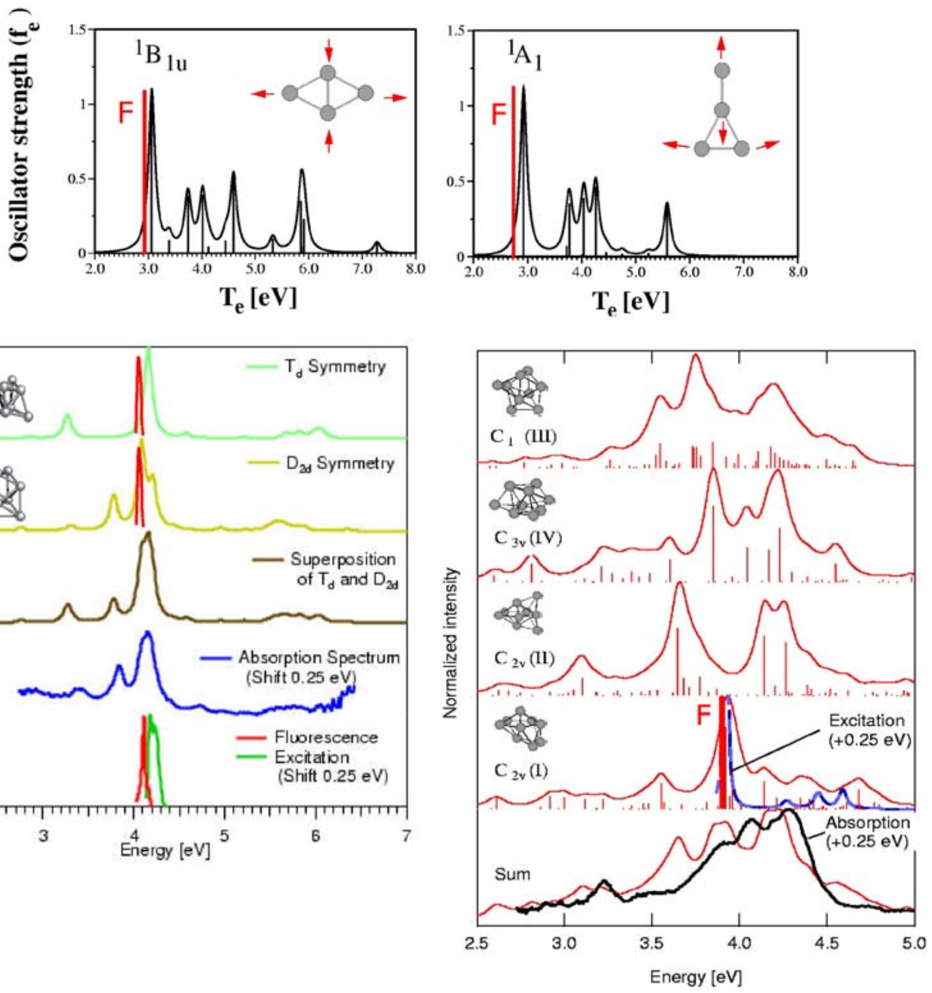

Fig. 3. Absorption spectra and positions of fluorescence bands for silver clusters of different sizes compared with experimental results for Ag_8 (bottom left) and Ag_9 (bottom right) shown in the lowest parts of the corresponding windows.

with two weakly bound CO_2, which can be easily released. Therefore under experimental conditions in which collisions with more than one CO molecule can occur the reaction should proceed due to cooperative effects.

Both above examples of silver and gold anionic clusters show the importance of cooperative effects for occurrence of strongly size selective reactions with O_2 and CO. The knowledge gained from the studies of cluster reactivity in the gasphase represents an important prerequisite to extend the investigation of the interplay with the surface, which is in progress.

2.2 Optical properties of silver clusters

Upon visible illumination of silver oxide films photoactivated fluorescence has been observed [21]. The photoinduced transformation was assumed to be due to generated silver clusters [22]. After local photocativation of the silver oxide films with blue or UV light (writing) the possibility to excite the fluorescence in the visible (readout) was proposed to be promising for advanced optical data storage [21,23].

We present here calculated optical spectra for different isomers of Ag_4, Ag_8 and Ag_9 clusters shown in Figure 3 obtained from ab initio random phase approximation (RPA) using 11-electron relativistic effective core potential (11e-RECP) with suitable AO basis set [24,25] which provide accurate description of excited states. They are characterized by one transition with dominant intensity. The strong dependence of the absorption spectra of the structures of the individual isomers is particularly pronounced for Ag_8 and Ag_9. They are compared with experimental results obtained in argon matrix [26] which include the shift by 0.25 eV to account the influence of the matrix. In order to determine the position of fluorescence band, geometry optimization of the excited state with the largest oscillatory strength has been carried out. The fluorescence band has been found for two isomers of Ag_4, two isomers of Ag_8 and for the energetically lowest lying isomer of Ag_9. The positions of these bands are only slightly lower with respect to the dominant transitions, indicating that the minima of the corresponding states lie close to Franck-Condon transitions. Comparison with experimental data [27,28] which are available for Ag_8 and Ag_9 show good agreement for excitation spectra and the position of fluorescence band in the case of the lowest energy isomers for both cases. Concerning recorded absorption spectra a mixture of isomers seems to be responsible for the measured features as can be depicted from Figure 3. There is

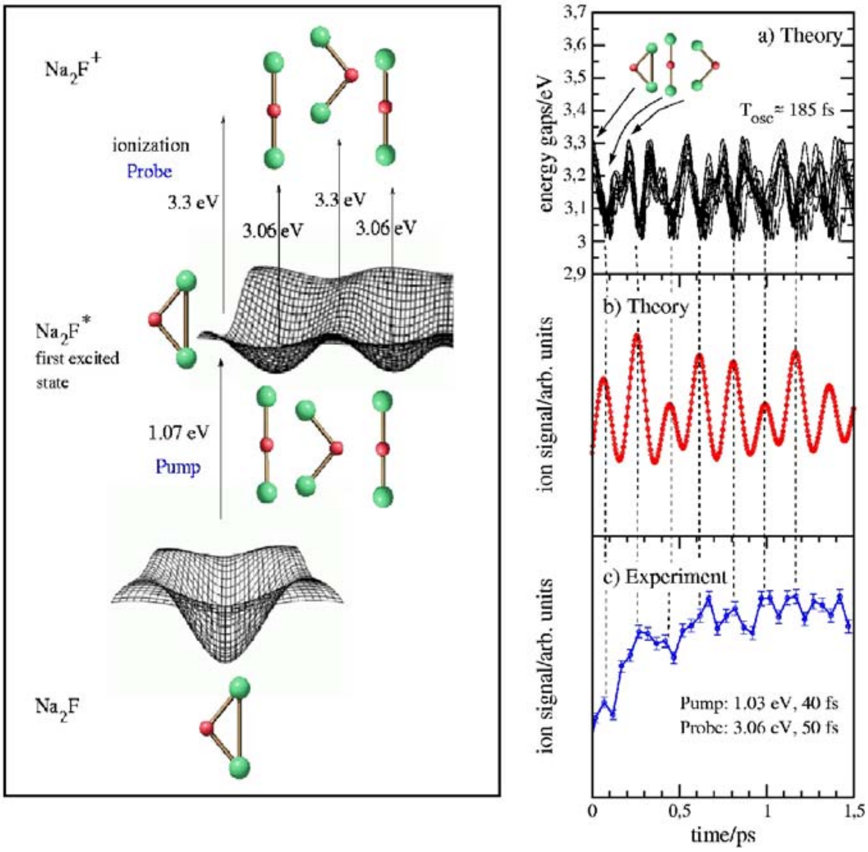

Fig. 4. Left side: electronic excitation scheme for the multistate dynamics of Na$_2$F indicating an oscillating butterfly-type geometric rearrangement after fs excitation of the first excited electronic state. Right side: (a) bunch of energy gaps between the first excited electronic state of Na$_2$F and the cationic ground state; (b) simulated pump-probe signal with (c) the experimentally obtained transient.

no doubt that small silver clusters fluoresce [27–29]. It is still an open question how are the silver clusters produced from silver oxide films and how the fluorescence can be caged in small silver or/and silver oxide particles to be useful for applications concerning optical storage.

2.3 Analysis and control of ultrafast processes

Femtosecond spectroscopy became a powerful tool for probing and controlling of real-time dynamics in molecules and clusters [30–33]. Advances in theoretical treatments, in particular a combination of Wigner approach to nuclear dynamics with ab initio adiabatic and nonadiabatic multistate dynamics "on the fly" [34–36] for all degrees of freedom (without precalculation of energy surfaces) allow for accurate simulation of pump-probe signals and for development of new control strategy for complex systems [37] as it will be shown below. Two approximations are introduced in the ab initio Wigner distribution approach: (a) perturbation series in the field limits applicability to the weak fields and (b) semiclassical treatment of nuclei requires averaging over ensemble of trajectories. Consequently, the quantum effects such as tunneling, zero point vibrational energy and interference phenomena cannot be described. However, quantum corrections are possible which account for the quantum dynamical effects [38] although these aspects are in development stage.

Nonstoichiometric sodium fluoride clusters Na$_n$F$_{n-1}$ offer a good opportunity to study real-time dynamics in the low lying electronically excited states, since one excess electron is strongly localized and therefore gives rise to intense absorption in the infrared regime [35,36,39,41]. Moreover, a large variety of ultrafast processes can be investigated as a function of the cluster size (each atom counts). This will be shown on the examples of Na$_2$F and Na$_3$F$_2$ in which metallic and/or ionic bond breaking as well as geometric relaxation through conical intersection occurs. In the latter case (Na$_3$F$_2$) the new strategy for obtaining of tailored laser pulses [37] in complex systems will be used to control the photoisomerization process.

Simulations of the fs pump-probe signals of Na$_2$F has been carried out in the framework of ab initio Wigner distribution approach according to the scheme given on Figure 4. This involves the generation of initial conditions by sampling of temperature dependent canonical Wigner distribution, the ab initio molecular dynamics (MD) in the excited electronic state and the calculation of the energy gaps between this state and the cationic ground state. For the calculations of excited states we use frozen ionic bond approximation which considers the excitation of the single excess-electron in the effective field of other $n-1$ valence electrons forming ionic bonds, since it provides accurate results at low computational demand [35]. Assuming short pulses (Gaussian pulse envelopes) the analytic expression for the pump-probe signal contains three exponentials corresponding to (i) Franck-Condon pump window, (ii) the probe window determined by the excited-neutral and ground-cationic energy gaps, and (iii) the resolution given by the duration of the pump and probe pulses. The calculation of the signals requires summation over the entire phase space.

The theoretical and experimental results [40] are presented in Figure 4. From the bunch of the time-dependent energy gaps a periodic relaxation dynamics with a period of ∼185 fs can be clearly identified. This period corresponds to half of the bending mode period in the first excited state. The maxima of the energy gaps correspond to the bent and the minima to the linear geometries (cf. left part of Fig. 4). At later times the gaps start to diverge due to the anharmonicities in the bending mode. The same oscillation period is also present in the pump-probe signal. For the probe pulse energy of 3.06 eV the maxima in the pump-probe signal correspond to the linear geometry which appears periodically due to the butterfly-like relaxation dynamics involving triangular and linear structure (cf. left part of Fig. 4). It should be pointed out that although the metallic bond breaking occurs in the excited state no further bond breakings or fragmentation occurs due to very strong ionic bonds which remain preserved. Experimental pump-probe signal [40] shown in the lower part of Figure 4 is in a very good agreement with the simulated signal. Our theoretical simulations have been also reproduced by full quantum dynamical simulations confirming the accuracy of the classical Wigner distribution approach [41]. This gave us the confidence to extend the applications to larger systems in which tailored laser fields can be used to control the processes.

Several control schemes exploiting the coherent properties of the laser fields have been proposed in the past [42,43,46]. Particularly suitable for the control of the isomerization is the Tannor-Rice pump-dump control scheme [42,44] which takes the advantage of differences in potential energy surfaces of different electronic states and uses the time delay between the pump and dump pulses as a parameter for control. Later, the original scheme was extended by using the optimal control theory [45] allowing to design pulses driving the system to the desired target with maximal yield. Central issue for the controllability of complex systems within the Tannor-Rice scheme [42,44,45] is the existence of a connective pathway between the initial state and the objective involving several electronic states. Based on our Wigner distribution approach [34–36], we have developed a new strategy for optimal control in complex systems [37] based on the concept of the intermediate target. The role of the intermediate target is to insure the connective pathway between the initial state and the objective and its existence can serve as a criterion for the controllability of complex systems. This will be illustrated below.

As shown in our previous work, the isomerization through conical intersection between the first excited state and ground state in Na_3F_2 is unselective and leads to equal population of both ground state isomers due to the large excess of internal energy gained during the dynamics on the first excited state [36]. Therefore, Na_3F_2 represents a challenging system on which our strategy for optimal control based on the concept of the intermediate target can be applied. For this purpose, an initial ensemble has been generated and propagated on the first excited state. In order to determine the intermediate target and the optimal time delay for the dump-pulse, the ensemble has been dumped to the ground states in regular time steps of 25 fs and subsequently propagated in the ground state. The objective (isomer II) is reached by the ensemble at $t_d = 250$ fs leading to the residence time longer than 500 fs. The ensemble corresponding to the intermediate target is shown in the upper part of Figure 5. The optimal pump and dump pulses have been calculated by solving decoupled integral equations of the Fredholm type and are also shown in the upper part of Figure 5. The decoupling of equations for optimal pulses is an advantage of our strategy which allows applications on complex systems at low computational demand. The pump pulse consists of two portions of ∼70 fs and ∼10 fs while the dump pulse is very short ∼20 fs and leads to almost instantaneous depopulation of the excited state at the optimal time delay. Furthermore, the spectral analysis of the optimal pulse has revealed that the pump pulse excites low lying modes which lead to the opening of the ionic Na_2F_2 cage and prepares the system for the isomerization. In conclusion, using the concept of the intermediate target we were able to show that the

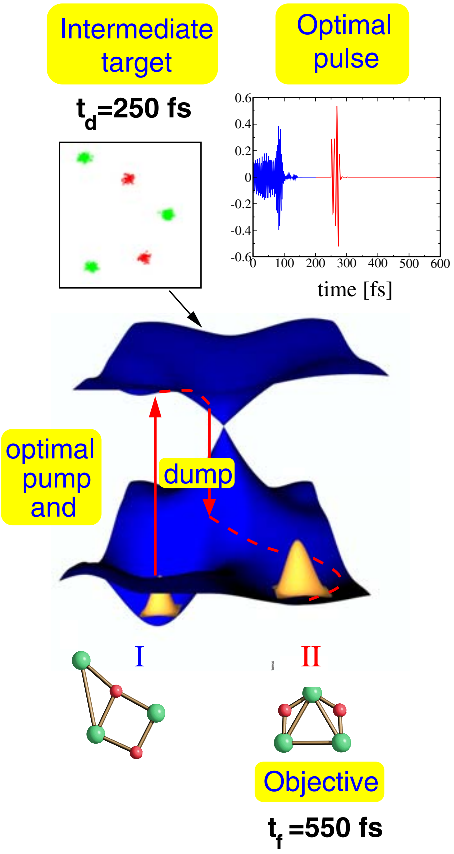

Fig. 5. Scheme for the pump-dump optimal control in the Na_3F_2 cluster with geometries of the two ground state isomers and the intermediate target (upper left part), and the optimal electric field corresponding to the pump and dump pulses (upper right part).

isomerization process can be driven to the desired objective while the nonselective radiationless transition through conical intersection can be suppressed. Moreover, through the analysis of the molecular dynamics the pulse shapes can be interpreted and connection between the dynamics and the pulse shapes can be established. In the future we will extend applications of our new strategy for control in two main directions: (i) the control of cluster reactivity (e.g. noble metal clusters) and (ii) control of conformational dynamics in biomolecules (e.g. aromatic aminoacids).

In summary we have shown that structures, size and laser fields can be used to tune chemical reactivity and stationary as well as real-time optical properties of clusters in the regime in which each atom counts.

This work was supported by the Deutsche Forschungsgemeinschaft SFB 450 “Analysis and Control of Photoinduced Ultrafast Reactions” and SPP 1153 “Clusters at Surfaces: Electron Structure and Magnetism”. We acknowledge close cooperation with experimental groups of Prof. L. Wöste, Freie Universität Berlin, Prof. A.W. Castleman Jr, Penn State University and Prof. C. Félix, EPFL Lausanne, which substantionally contributed to the presented results.

References

1. V. Bonačić-Koutecký, P. Fantucci, J. Koutecký, Chem. Rev. **91**, 1035 (1991)
2. A.W. Castleman Jr, K.H. Bowen, J. Phys. Chem. **100**, 12911 (1996)
3. J. Jortner, Faraday Discuss. **108**, 1 (1997)
4. U. Landman, Int. J. Mod. Phys. B **6**, 3623 (1992)
5. M. Haruta, Catalysis Today **36**, 153 (1997)
6. A. Sanchez, S. Abbet, U. Heiz, W.-D. Schneider, H. Häkkinen, R.N. Barnett, U. Landman, J. Phys. Chem. A **103**, 9573 (1999)
7. W.T. Wallace, R.L. Whetten, J. Am. Chem. Soc. **124**, 7499 (2002)
8. A.D. Becke, Phys. Rev. A **38**, 3098 (1988)
9. A.D. Becke, J. Chem. Phys. **98**, 5648 (1993)
10. C. Lee, W. Yang, R.G. Parr, Phys. Rev. B **37**, 785 (1988)
11. J.P. Perdew, Y. Wang, Phys. Rev. B **45**, 13244 (1992)
12. W.T. Wallace, R.B. Wyrwas, R.L. Whetten, R. Mitrić, V. Bonačić-Koutecký, J. Am. Chem. Soc. **125**, 8408 (2003)
13. M.L. Kimble, A.W. Castleman Jr, R. Mitrić, C. Bürgel, V. Bonačić-Koutecký, J. Am. Chem. Soc. **126**, 2526 (2004)
14. J. Hagen, L.D. Socaciu, J. Le Roux, D. Popolan, T.M. Bernhardt, L. Wöste, R. Mitrić, H. Noack, V. Bonačić-Koutecký, J. Am. Chem. Soc. **126**, 3442 (2004)
15. B. Yoon, H. Häkkinen, U. Landman, J. Phys. Chem. A **107**, 4066 (2003)
16. L.D. Socaciu, J. Hagen, T.M. Bernhardt, L. Wöste, U. Heiz, H. Häkkinen, U. Landman, J. Am. Chem. Soc. **125**, 10437 (2003)
17. A. Franceschettei, S.J. Pennycook, S.T. Pantelides, Chem. Phys. Lett. **374**, 471 (2003)
18. Q. Sun, P. Jena, Y.D. Kim, M. Fischer, G. Ganteför, J. Chem. Phys. **120**, 6510 (2004)
19. M.L. Kimble, A.W. Castleman Jr, C. Bürgel, R. Mitrić, V. Bonačić-Koutecký, J. Am. Chem. Soc. (submitted)
20. Note that the lowest energy structures of AgO_2^- and $Ag_3O_4^-$ contain dissociated oxygen (not shown), which requires considerable activation energy not available under experimental conditions involving molecular oxygen
21. L.A. Peyser, A.E. Vinson, A.P. Bartko, R.M. Dickson, Science **291**, 103 (2001)
22. L.A. Peyser, T.H. Lee, R.M. Dickson, J. Phys. Chem. B **106**, 7725 (2002)
23. T. Gleitsmann, B. Stegemann, T.M. Bernhardt, Appl. Phys. Lett. **84**, 4050 (2004)
24. V. Bonačić-Koutecký, J. Pittner, M. Boiron, P. Fantucci, J. Chem. Phys. **110**, 3876 (1999)
25. V. Bonačić-Koutecký, V. Veyret, R. Mitrić, J. Chem. Phys. **115**, 10450 (2001)
26. S. Fedrigo, W. Harbich, J. Buttet, Phys. Rev. B **47**, 10706 (1993)
27. C. Sieber, J. Buttet, W. Harbich, C. Félix, R. Mitrić, V. Bonačić-Koutecký, Phys. Rev. A **70**, 041201 (2004)
28. C. Félix, C. Sieber, W. Harbich, J. Buttet, I. Rabin, W. Schulze, G. Ertl, Phys. Rev. Lett. **86**, 2992, (2001)
29. L. König, I. Rabin, W. Schulze, G. Ertl, Science **274**, 1353 (1996)
30. A.H. Zewail, *Femtochemistry* (World Scientific, Singapore, 1994)
31. *Femtosecond Chemistry*, edited by J. Manz, L. Wöste (VCH Verlagsgesellschaft mbH, Weinheim, Germany, 1995), Vols. 1 and 2
32. A.H. Zewail, J. Phys. Chem. A **104**, 5660 (2000)
33. T. Brixner, G. Gerber, Chem. Phys. Chem. **4**, 418 (2003)
34. M. Hartmann, J. Pittner, V. Bonačić-Koutecký, A. Heidenreich, J. Jortner, J. Chem. Phys. **108**, 3096 (1998)
35. M. Hartmann, J. Pittner, V. Bonačić-Koutecký, J. Chem. Phys. **114**, 2106 (2001)
36. M. Hartmann, J. Pittner, V. Bonačić-Koutecký, J. Chem. Phys. **114**, 2123 (2001)
37. R. Mitrić, M. Hartmann, J. Pittner, V. Bonačić-Koutecký, J. Phys. Chem. A **106**, 10477 (2002)
38. A. Donoso, C.C. Martens, Phys. Rev. Lett. **87**, 223202 (2001)
39. V. Bonačić-Koutecký, J. Pittner, Chem. Phys. **225**, 173 (1997)
40. S. Vajda, C. Lupulescu, A. Merli, F. Budzyn, L. Wöste, M. Hartmann, J. Pittner, V. Bonačić-Koutecký, Phys. Rev. Lett. **89**, 213404 (2002)
41. M.C. Heitz, G. Durand, F. Spiegelman, C. Meier, J. Chem. Phys. **118**, 1282 (2003)
42. D.J. Tannor, S.A. Rice, J. Chem. Phys. **83**, 5013 (1985)
43. M. Shapiro, P. Brumer, J. Chem. Phys. **84**, 4103 (1986)
44. J. Tannor, R. Kosloff, S.A. Rice, J. Chem. Phys. **85**, 5805 (1986)
45. R. Kosloff, S.A. Rice, P. Gaspard, S. Tersigni, D.J. Tannor, Chem. Phys. **139**, 201 (1989)
46. A.P. Peirce, M.A. Dahleh, H. Rabitz, Phys. Rev. A **37**, 4950 (1988)